Available online at www.sciencedirect.com

ScienceDirect

Procedia Structural Integrity 42 (2022) 838–846

Structural Integrity Procedia

www.elsevier.com/locate/procedia

23 European Conference on Fracture - ECF23

High Temperature Mechanical Properties of AlMgScZr Alloy Produced by Laser Powder Bed Fusion

Maria Beatrice Abrami[a]*, Marialaura Tocci[a], Marcello Gelfi[a], Annalisa Pola[a]

[a]*University of Brescia, Department of Mechanical and Industrial Engineering, via Branze 38, 25124 Brescia, Italy*

Abstract

The present work is focused on the fracture behavior of Scalmalloy®, an AlMgScZr alloy specifically developed for laser powder bed fusion (L-PBF) process. This material has gained increasing attention for applications requiring high performances due to its outstanding properties and low anisotropic behavior. The responsible for the high specific properties of the alloy is its microstructure, characterized by fine grains and the presence of $Al_3(Sc,Zr)$ precipitates as well as nano-sized oxides. These particles form during the L-PBF process and act as nucleation sites for grain refinement. They have been also found to exhibit relevant thermal stability. An increase in strength is achieved from the further formation of smaller $Al_3(Sc,Zr)$ precipitates during the annealing treatment at 325 °C, which is a typical post treatment for this alloy.
The fracture mechanism of AlMgScZr alloy has rarely been studied so far, especially at high temperature or after high temperature exposure. In the present work, samples were produced via L-PBF and annealed. Tensile tests were then performed at different testing temperatures, i.e. 25 °C, 100 °C, 150 °C. Furthermore, samples were tested both under annealed condition and after soaking at 100 °C, 150 °C, 200 °C for 10 h. Mechanical properties were evaluated, and the fracture surface morphology was observed under scanning electron microscope to analyze the failure mechanism. Differential scanning calorimetry analyses were also performed to verify the thermal stability of precipitates. The correlation between these results and the mechanical properties allowed the investigation of the fracture behavior evolution with temperature. This provided a comprehensive characterization of the high temperature mechanical properties of AlMgScZr alloy, useful for evaluating new high temperature applications.

Keywords: Scalmalloy®; High temperature behavior; Additive Manufacturing

* Corresponding author. Tel.: +39-0303715826; fax: +39-0303702448.
E-mail address: m.abrami003@unibs.it

10.1016/j.prostr.2022.12.106

1. Introduction

Laser powder bed fusion (L-PBF) process is an additive manufacturing (AM) technique which consists in manufacturing components by selectively melting a powder bed and adding material layer by layer. The extremely high cooling rates involved (10^4-10^6 K/s) allow the obtainment of fine microstructures resulting in high performances, thus making it the most widely used AM method (DebRoy et al. 2018). Some of the latest progresses of L-PBF concern the development of special alloys specifically tailored for the process (Sing and Yeong 2020, Aversa et al. 2019). Among them, aluminum alloys are widely studied due to the increasing need to manufacture high-performance components combined with low density for applications in the automotive or aerospace fields. In fact, the high-strength Al alloys manufactured with traditional methods (2xxx, 7xxx) have revealed some problems with AM, such as solidification cracking, evaporation of volatile elements and anisotropy in the final component (Sing and Yeong 2020, Aversa et al. 2019). On the other hand, the most common Al alloys used for L-PBF, e.g. AlSi10Mg, present some limits mainly related to the anisotropy and the strength properties, which do not reach those of the high-strength conventional Al alloys previously mentioned.

To meet the growing industrial requirements, Scalmalloy® (AlMgScZr alloy) has been specifically developed for L-PBF process by Airbus, with the aim of fully taking advantage of the process benefits combined to the high strength properties of the material. The latter are the result of the peculiar microstructure of the alloy, which is characterized by the presence of Al_3(Sc,Zr) precipitates and fine-dispersed Al-Mg oxides with different compositions, arising mainly from the oxide layer that covers the powder and breaks up during laser scanning (Spierings et al. 2016). Both these types of particles strengthen the matrix and act as nucleation sites for grain refinement. In fact, Scalmalloy® consists in fine grain regions (150 nm ÷ 1 μm) located along the melt pool boundaries, alternated to columnar grain regions (2 ÷ 15 μm) within the melt pools (Spierings et al. 2017a, Zhai et al. 2022, Isaac et al. 2021, Mehta, Svanberg and Nyborg 2022, Spierings et al. 2017b, Croteau et al. 2018). Primary Al_3(Sc, Zr) particles predominantly form on grain boundaries, while the typical post treatment (325 °C, 4 h) leads the further formation of nano-sized precipitates also inside the matrix. This results in the strengthening of the alloy, as well as low anisotropic behaviour of the component. In addition, the presence of Zr decreases the solidification range of Al alloys, thus reducing the solidification cracking tendency and facilitating the manufacturing with L-PBF (Zhang et al. 2017).

The characterization of Scalmalloy® behavior at high temperatures has rarely been carried out so far (Bi et al. 2022, Abrami et al. 2021), however, it is highly interesting in order to open new fields of application to this alloy. To fill this literature gap, the present work aims at investigating the tensile mechanical properties at high temperatures (up to 150 °C) of AlMgScZr alloy in both annealed condition and after high temperature exposures (up to 200 °C). In addition, the failure mechanism of the alloy was identified by examining the fracture surfaces under the scanning electron microscope (SEM), while the thermal stability of precipitates was studied by performing differential scanning calorimetry (DSC) analyses.

2. Experimental procedure

In the present study, AlMgScZr (Scalmalloy®) powder was used for samples manufacturing. The nominal chemical composition of the powder was Al-4.5Mg-0.7Sc-0.3Zr (in wt%).

AlMgScZr dumbbell specimens for tensile tests were produced via L-PBF process by using an EOS M 290 machine with the following parameters: laser power of 370 W, laser scan speed of 130 cm/s, hatch spacing of 90 μm, layer thickness of 30 μm and spot size of 100 μm. Specimens were manufactured with two different building orientations to analyze their effect on the tensile behavior. In detail, half of the samples were horizontally built (named "H-samples"), and the other half vertically built (named "V-samples"), as displayed in Fig. 1 together with their sizes. After manufacturing, samples were annealed at 325 °C for 4 hours and then machined to final size.

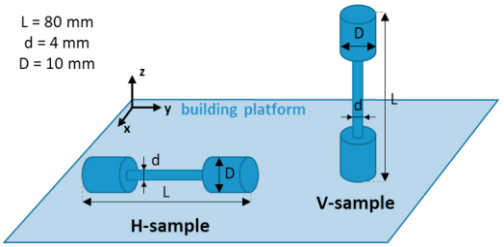

Fig. 1. Representation of the dumbbell samples: H-sample and V-sample.

Tensile tests were carried out using a Instron mod. 3369 machine (50 kN) with a crosshead speed fixed at 1 mm/min up to 5% of deformation and then at 2 mm/min up to break. Table 1 summarizes the investigated tensile test conditions. In detail, samples were tested both in the as-annealed conditions and after soaking at high temperatures, i.e. 100, 150 and 200 °C, for 10 hours before testing. For better clarity, the conditions of samples before tensile testing are indicated with numbers from 1 to 4. Moreover, to provide a detailed overview on the AlMgScZr high temperature behavior, the tensile tests were performed at three different temperatures, i.e. 25, 100 and 150 °C, indicated as room temperature (RT), medium temperature (MT) and high temperature (HT), respectively. Every analyzed condition implies tests on both H and V samples with 3 repetitions. For samples tested in the as-annealed conditions, the soaking time in temperature was of 0.1 hours to ensure isothermal condition of the sample.

Table 1. Tensile test conditions and designation.

			Testing temperature		
			RT	**MT**	**HT**
			25 °C	**100 °C**	**150 °C**
Condition before testing	**1**	**As-annealed**	✓	✓	✓
	2	**Annealed** + soaked at **100 °C** for 10 h	✓	✓	
	3	**Annealed** + soaked at **150 °C** for 10 h	✓		✓
	4	**Annealed** + soaked at **200 °C** for 10 h	✓		

Microstructural analyses were performed on samples in the annealed state and after the exposure for 10 hours to the highest temperature (i.e. 200°C). Samples for metallographic investigations were obtained from the reduced section of tensile specimens, cold resin mounted and polished up to mirror finish using silicon carbide abrasive papers (P800, P1000 and P1200) followed by 3 and 1 μm diamond suspension for fine polishing. Subsequently, samples were chemically etched to reveal the microstructure using a phosphoric acid solution (10% H_2PO_4) heated to 50 °C for 8 min. The microstructural analysis was carried out with the LEICA DMI 5000M microscope.

To investigate the failure mechanism, fracture surface analyses were carried out with the scanning electron microscope (SEM) Leo Evo 40XVP on samples representing the extreme conditions of tensile tests, i.e. those marked in red in Table 1 (1.RT, 4.RT, 1.HT, 3.HT).

Finally, differential scanning calorimetry (DSC) analyses were carried out on as-annealed samples to check any microstructural variation with temperature and, to deeply investigate the precipitation evolution, the results were also compared to those of an as-built sample, i.e. examined before annealing. The DSC tests were carried by heating the sample with a controlled ramp of 20 °C/min up to 400 °C.

3. Results and discussion

3.1. Microstructural analysis

The micrographs collected from the abovementioned samples along both the building direction (z) and the direction parallel to the deposited layers (xy) are shown in Fig. 2.

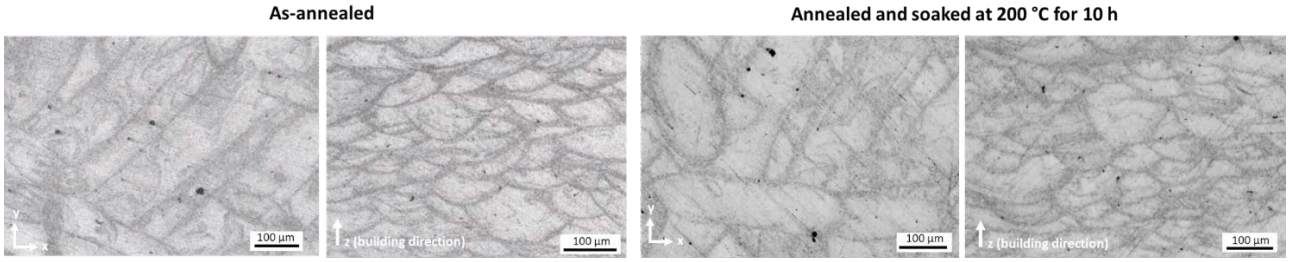

Fig. 2. Comparison between micrographs of samples in the as-annealed condition and after soaking at 200 °C.

Both the samples show the typical structure arising from L-PBF, i.e. scan tracks reflecting the laser path in the xy surface and melt pools overlapping each other along the z direction. As typical of Al alloys, melt pools show a very wide shape, due to their good thermal conductivity (Spierings et al. 2017a). The permanence of this structure after annealing can be attributed to the relative low temperature of the heat treatment that can be considered as a stress-relief annealing, where the texture as well as the crystallographic orientation of grains are not expected to change from the as-built condition (Nezhadfar et al. 2021). On the other side, the similarity of micrographs for the two analysed conditions points out the stability of Scalmalloy® microstructure even at temperature of 200 °C.

3.2. Mechanical properties

3.2.1. Room temperature tensile tests

Tensile test results for samples tested at 25 °C (RT cases) are displayed in Fig. 3. In detail, the ultimate tensile strength (UTS) and yield strength (YS) are reported, as well as the elongation at break (El), both for the H and V samples.

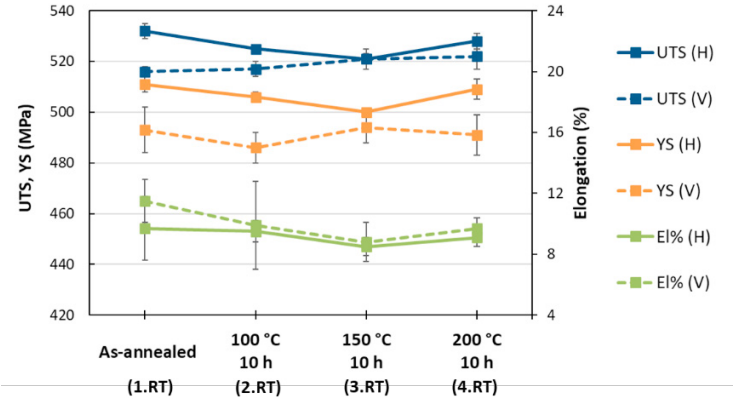

Fig. 3. Mechanical properties (UTS, YS and El) of H and V samples tested at RT (25 °C). Samples conditions are reported on the x axis.

The results confirm the high properties achievable by annealing Scalmalloy® at 325 °C for 4 hours (H-sample): UTS = 532 ± 3 MPa, YS = 511 ± 3 MPa, El = 10 ± 2 % Furthermore, they were found to be slightly higher than those recorded after 300 °C for 144 h (Bi et al. 2022), thus highlighting that excellent results are achievable even with a shorter heat treatment performed at a slightly higher temperature.

In the annealed condition, the mechanical properties of Scalmalloy® remains stable even if the material is exposed to temperatures up to 200 °C for several hours. In fact, for the H-samples the maximum deviations between the as-annealed state and after soaking at 200 °C are of 11 MPa for both YS and UTS, and of 1% for El. For V-samples, UTS and YS after soaking deviate of maximum 7 and 6 MPa, respectively, while El of 3%.

Furthermore, H-samples exhibits slightly better tensile strength properties than the V ones, together with lower El. This can be attributed to the higher cooling rates, as well as the lower amount of melt pool boundaries in the load bearing surface, which discourages the propagation of the crack, typically nucleating and propagating through the melt pool boundaries (Palmeri et al. 2021, Xiong et al. 2019, Zhao et al. 2018, Pellizzari et al. 2020).

3.2.2. Medium and high temperature tensile tests

The results of the tests carried out at MT and HT on the as-annealed samples are displayed in Fig. 4 and compared to those carried out at RT (cases 1: 1.RT, 1.MT, 1.HT). As expected, strength properties worsen as temperature increases, while the elongation improves. In detail, YS at 150 °C decreased of 25% (V-samples) and 30% (H-samples), while UTS dropped by 25% (V-samples) and 28% (H-samples) compared to their original properties at RT. Nevertheless, the recorded values are still higher than those typical of standard Al alloys that are presented in the next paragraph.

By comparing results of H and V samples, no significant changes are observed, denoting a greater effect of the testing temperature rather than the building orientation. This may be due to different factors, as gas-porosity enlargement during the test, thermal effects or precipitates modifications, which thus can deteriorate mechanical properties. To better investigate the weakening mechanism, SEM and DSC analyses were performed and the corresponding results are reported in Paragraph 3.3 and 3.4, respectively.

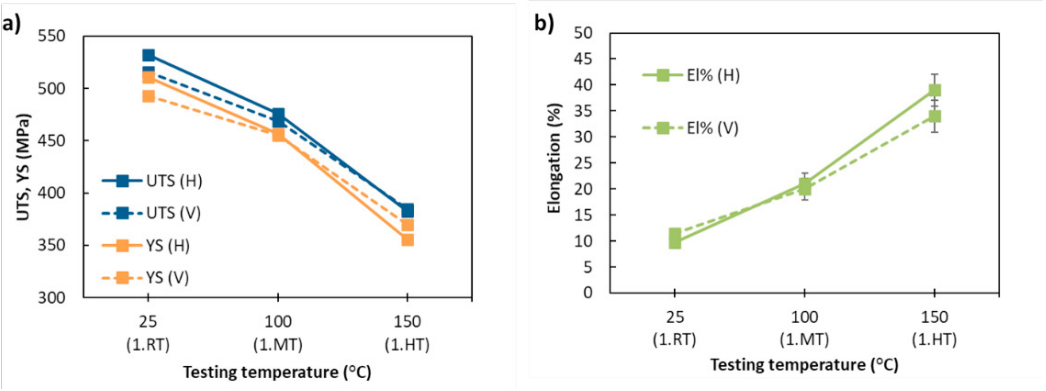

Fig. 4. a) UTS, YS and b) El of the as-annealed samples as function of the different testing temperatures.

The results of the tests performed on samples soaked at the testing temperature for 10 hours before testing are shown in Fig. 5 and compared to those carried out at RT (cases 1.RT, 2.MT, 3.HT). By comparing Figs. 4 and 5, it is confirmed that also the hot tensile properties of the annealed Scalmalloy® remain constant for soaking temperatures lower than 200 °C.

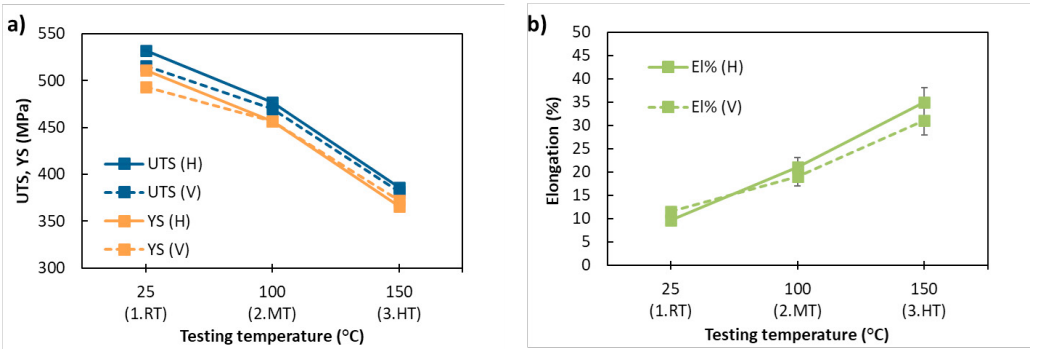

Fig. 5. a) UTS, YS and b) El of the samples tested at different testing temperatures after soaking.

3.2.3. Comparison with other Al alloys

Fig. 6 shows the comparison between YS and UTS at high testing temperatures of Scalmalloy® (H-samples) and other Al alloys, i.e. additive manufactured AlSi10Mg both in as-built (Tocci et al. 2021) and stress-relieved (Uzan et al. 2018) conditions and AlSi9Cu3 cast (Zamani, Seifeddine and Jarfors 2015). In detail, AlSi10Mg was chosen as it is the most widely used Al alloy for AM, while AlSi9Cu3 cast as is commonly employed for high temperature applications. It is evident that Scalmalloy® has higher mechanical properties than the other considered Al alloys, thus confirming its potential for high temperature applications.

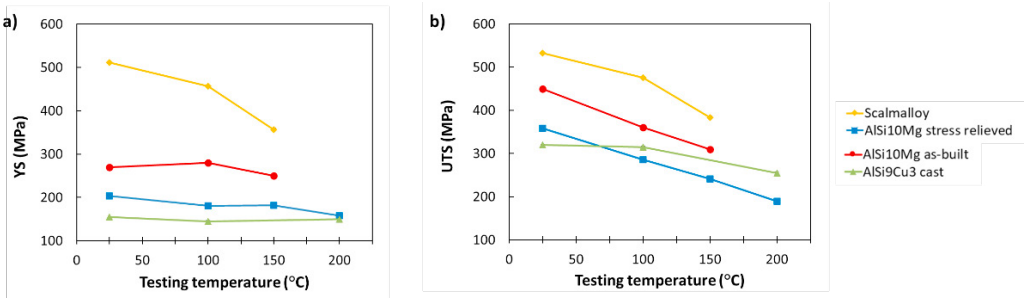

Fig. 6. Comparison between high temperature properties of Scalmalloy® and other Al alloys: a) YS and b) UTS.

3.3. Fractography

The fracture surface of the abovementioned samples (1.RT, 4.RT, 1.HT, 3.HT) were analysed at the Scanning Electronic Microscope (SEM). Since the building orientation did not show significant differences, only H-samples were considered, as those exhibiting slightly higher mechanical properties.

Results of SEM analyses of samples tested at 25 °C (1.RT, 4.RT) are shown in Fig. 7, while Table 2 reports the corresponding EDS analyses. Necking is comparable for the as-annealed case and after soaking at 200 °C for 10 h (Figs. 7a, 7e), as well as the fracture surfaces. In fact, the latter appear as rough and full of micro-cavities, which can be linked both to already existing porosities and dimples. Dimples represent the typical features of ductile fractures and are caused by the deformation of the matrix localized around second phases (second-phase particles, non-metallic inclusions, etc.) (Xiong et al. 2019, Gao et al. 2020). The particles responsible for dimples nucleation can be identified as oxides, some constituted only by Al and Mg, and some other richer in Sc (Figs. 7c, 7g, Table 2), which previously formed during the L-PBF process. In fact, they derive from powder oxidation as well as from the layer which oxidates during process and is subsequently remelt several times generating oxide particles (Spierings et al. 2017a).

At higher magnification (Figs. 7d, 7h), very fine dimples can be found for both samples, which constitutes the flat areas found at lower magnifications. These flat regions experienced lower plastic deformation, and it is likely from these that fracture nucleated and propagated (Li et al. 2016, Xiong et al. 2019). Moreover, it is possible to detect the presence of very thin particles inside the micro-dimples, too small to be analysed by EDS microprobe (see yellow arrows in Figs. 7d, 7h). Their uniform distribution and the nano-sized dimensions suggest that they are probably the Al_3(Sc, Zr) particles and oxides typically found in the annealed Scalmalloy® (Spierings et al. 2017a, Croteau et al. 2018). Therefore, during tensile tests the stress concentration occurred at the interface between the matrix and these nano-sized particles thus forming micro-dimples. Then, their coalescence generated specimen fracture.

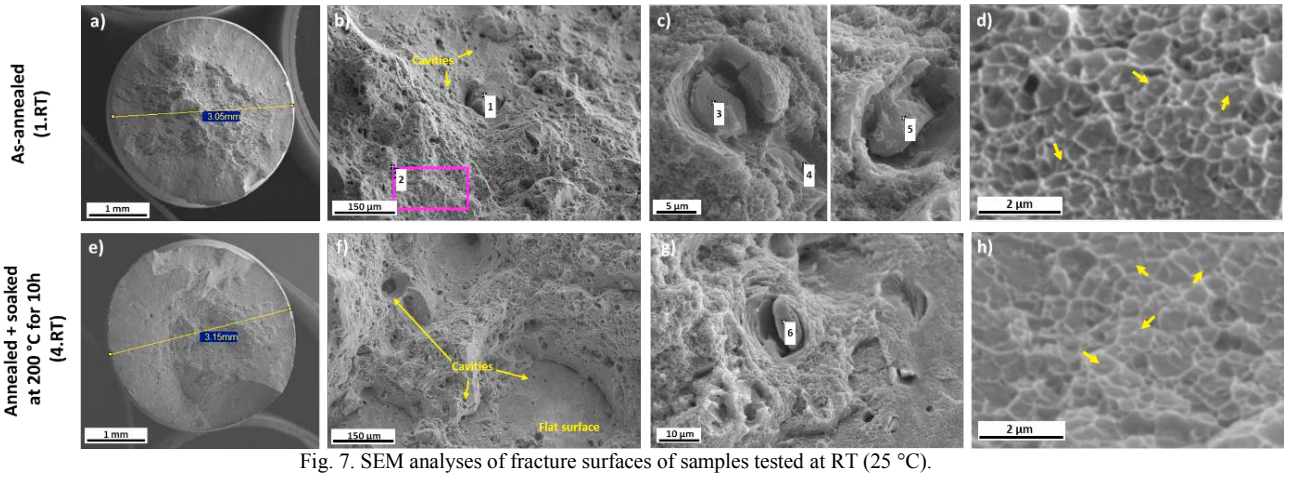

Fig. 7. SEM analyses of fracture surfaces of samples tested at RT (25 °C).

Table 2. EDS analyses (wt%) of areas indicated in Fig. 7.

	O	Mg	Al	Sc
1	-	3.91	95.96	0.12
2	-	4.16	95.02	0.82
3	45.93	2.54	41.37	10.16
4	31.06	3.58	63.13	2.22
5	6.88	4.26	88.86	-
6	48.63	4.41	38.07	8.89

Results of SEM analyses of samples tested at 150 °C (1.HT, 3.HT) are shown in Fig. 8, while Table 3 reports the corresponding EDS analyses. Necking increased respect to the RT tensile tests (Figs. 8a, 8e), denoting a more ductile behaviour of the samples. Fracture surfaces of the HT cases are similar to each other, and they appear richer of cavities than the RT-tested specimens, which is due to the high testing temperature that further promotes porosities enlargement. In this regard, the effect of the testing temperature is stronger than that of temperature soaking, as more evident differences can be seen by comparing RT to HT cases, rather than those tested at the same temperature but previously soaked, thus confirming what previously found during tensile tests. Oxides are found also for specimens tested at HT (Figs. 8c, 8g, Table 3), whose morphology and quantity of elements is essentially the same of the previous cases, thus confirming that their formation is linked to the L-PBF process.

Micro-dimples can be detected also in the HT cases at higher magnification (Figs. 8d, 8h). It must be noted that they appear as slightly larger than those found in RT-tested samples, thus determining the more ductile behaviour of the samples tested at HT. Furthermore, particles inside micro-dimples do not seem to change in size after HT exposures (Figs. 7d, 7h, 8d, 8h), thus revealing that the weakening of the alloy at HT may be attributed to predominantly thermal effects, as a greater mobility of dislocations, activation of recovery phenomena or thermal softening effects.

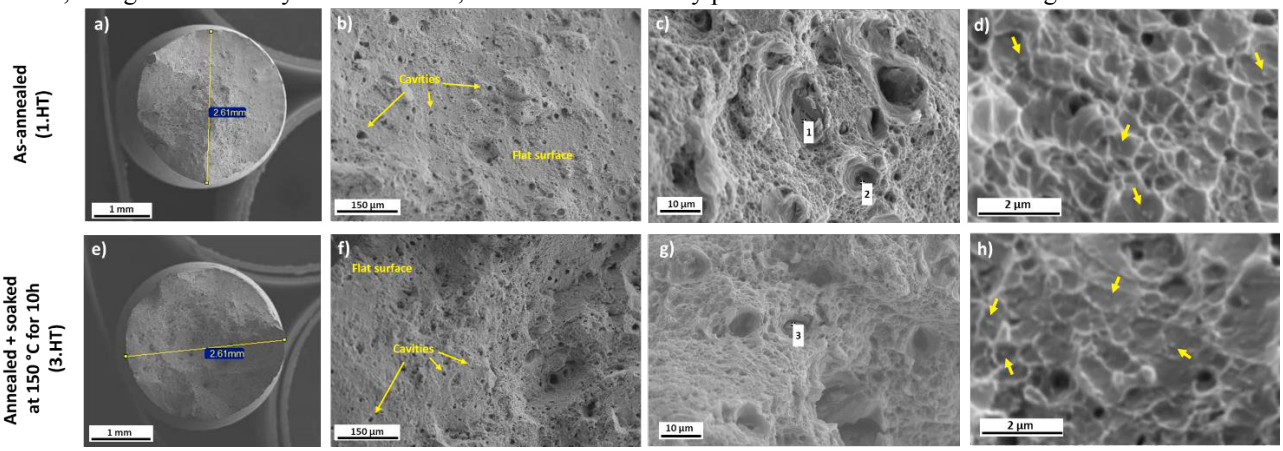

Fig. 8. SEM analyses of fracture surfaces of samples tested at HT (150 °C).

Table 3. EDS analyses (wt%) of areas indicated in Fig. 8.

	O	Mg	Al	Sc
1	42.33	2.43	45.21	10.03
2	-	-	100	-
3	42.32	3.73	48.07	4.89

3.4. DSC analysis

To verify the assumptions arising from the failure analysis, DSC analyses were performed on the as-built and as-annealed samples (Fig. 9). The onset temperature of 264.5 °C in the as-built sample is associated to the formation of $Al_3(Sc, Zr)$, in agreement with the heat treatment performed. The same phenomenon is instead not evident in the as-annealed sample. Also, no peaks due to dissolution or coarsening of precipitates were recorded in the as-annealed

sample, denoting that $Al_3(Sc, Zr)$ particles do not evolve with heating up to 400 °C, thus confirming the thermal stability of these particles after annealing.

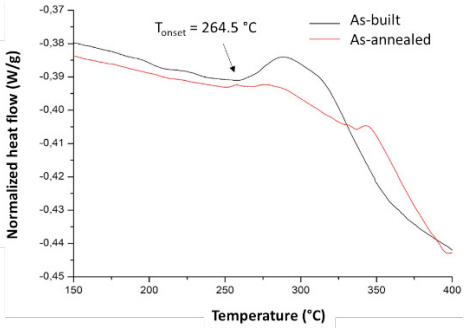

Fig. 9. DSC thermogram of as-built and as-annealed samples.

4. Conclusions

In this study, the high temperature mechanical properties of AlMgScZr alloy were investigated by performing different tests at high temperatures and after high temperatures soaking. The following conclusions can be drawn:

- Soaking in temperature up to 200 °C prior to test does not alter mechanical properties, both in the case of samples tested at room temperature and at high temperatures.
- The alloy fracture behavior is ductile and characterized by the formation of micro-dimples generated at the interface between matrix and particles, i.e. $Al_3(Sc, Zr)$ and oxides. These micro-dimples increase in size by increasing the testing temperature, while particles do not evolve. This points out that the loss of strength recorded as the testing temperature increases can be mainly ascribed to thermal effects concerning the Al-Mg matrix.
- Results show remarkable properties at high temperatures, especially if compared to other Al alloys, making Scalmalloy® suitable for applications at high temperatures in the range of 100-150 °C and after high temperature exposures up to 200 °C.

Acknowledgments

The Authors thank Dr. L. Girelli and MSc. Eng. F. Lollio for their contribution in experimental activities and Professor L. Battezzati and Dr. D. Gianoglio (University of Torino) for their support in the DSC analyses.

References

Abrami, M. B., Montesano, L., Tocci, M., Pola, A., Gelfi, M., 2021. High temperature wear behavior of AlMgScZr alloy produced by laser powder bed fusion. Procedia Structural Integrity, 878-886.

Aversa, A., Marchese, G., Saboori, A., Bassini, E., Manfredi, D., Biamino, S., Ugues, D., Fino P., Lombardi, M., 2019. New Aluminum Alloys Specifically Designed for Laser Powder Bed Fusion: A Review. Materials, 12.

Bi, J., Liu, L., Wang, C., Chen, G., Jia, X., Chen, X., Xia, H., Li, X., Starostenkov, M. D., Han, B., Dong, G., 2022. Microstructure, tensile properties and heat-resistant properties of selective laser melted AlMgScZr alloy under long-term aging treatment. Materials Science and Engineering A, 833.

Croteau, J. R., Griffiths, S., Rossell, M. D., Leinenbach, C., Kenel, C., Jansen, V., Seidman, D. N., Dunand, D. C., Vo, N. Q., 2018. Microstructure and mechanical properties of Al-Mg-Zr alloys processed by selective laser melting. Acta Materialia, 153, 35-44.

DebRoy, T., Wei, H. L., Zuback, J. S., Mukherjee, T., Elmer, J. W., Milewski, J. O., Beese, A. M., Wilson-Heid, A., De, A., Zhang, W., 2018. Additive manufacturing of metallic components – Process, structure and properties. Progress in Materials Science, 92, 112-224.

Gao, C., Wu, W., Shi, J., Xiao Z., Akbarzadeh, A. H., 2020. Simultaneous enhancement of strength, ductility, and hardness of TiN/AlSi10Mg nanocomposites via selective laser melting. Additive Manufacturing, 34.

Isaac, J. P., Lee, S., Shamsaei, N., Tippur, H. V., 2021. Dynamic fracture behavior of additively manufactured Scalmalloy®: Effects of build orientation, heat-treatment and loading-rate. Materials Science and Engineering A, 826.

Li, W., Li, S., Liu, J., Zhang, A., Zhou, Y., Wei, Q., Yan, C., Shi, Y., 2016. Effect of heat treatment on AlSi10Mg alloy fabricated by selective laser melting: Microstructure evolution, mechanical properties and fracture mechanism. Materials Science and Engineering A, 663, 116-125.

Mehta, B., Svanberg, A., Nyborg, L., 2022. Laser powder bed fusion of an Al-Mg-Sc-Zr alloy: Manufacturing, peak hardening response and thermal stability at peak hardness. Metals, 12.

Nezhadfar, P. D., Thompson, S., Saharan, A., Phan, N., Shamsaei, N., 2021. Structural integrity of additively manufactured aluminum alloys: Effects of build orientation on microstructure, porosity, and fatigue behavior. Additive Manufacturing, 47.

Palmeri, D., Buffa, G., Pollara, G., Fratini, L., 2021. The Effect of Building Direction on Microstructure and Microhardness during Selective Laser Melting of Ti6Al4V Titanium Alloy. Journal of Materials Engineering and Performance, 30**,** 8725-8734.

Pellizzari, M., AlMangour, B., Benedetti, M., Furlani, S., Grzesiak, D., Deirmina, F., 2020. Effects of building direction and defect sensitivity on the fatigue behavior of additively manufactured H13 tool steel. Theoretical and Applied Fracture Mechanics, 108**,** 102634.

Sing, S. L., Yeong, W. Y., 2020. Laser powder bed fusion for metal additive manufacturing: perspectives on recent developments. Virtual and Physical Prototyping, 15**,** 359-370.

Spierings, A. B., Dawson, K., Heeling, T., Uggowitzer, P. J., Schäublin, R., Palm, F., Wegener, K., 2017a. Microstructural features of Sc- and Zr-modified Al-Mg alloys processed by selective laser melting. Materials and Design, 115**,** 52-63.

Spierings, A. B., Dawson, K., Kern, K., Palm, F., Wegener, K., 2017b. SLM-processed Sc- and Zr- modified Al-Mg alloy: Mechanical properties and microstructural effects of heat treatment. Materials Science and Engineering A, 701**,** 264-273.

Spierings, A. B., Dawson, K., Voegtlin, M., Palm, F., Uggowitzer, P. J., 2016. Microstructure and mechanical properties of as-processed scandium-modified aluminium using selective laser melting. CIRP Annals - Manufacturing Technology, 65**,** 213-216.

Tocci, M., Varone, A., Montanari R., Pola, A., 2021. Study of high temperature properties of AlSi10Mg alloy produced by laser-based powder bed fusion. In Materials Science Forum, 1485-1491.

Uzan, N. E., Shneck, R., Yeheskel, O., Frage, N., 2018. High-temperature mechanical properties of AlSi10Mg specimens fabricated by additive manufacturing using selective laser melting technologies (AM-SLM). Additive Manufacturing, 24**,** 257-263.

Xiong, Z. H., Liu, S. L., Li, S. F., Shi, Y., Yang, Y. F., Misra, R. D. K., 2019. Role of melt pool boundary condition in determining the mechanical properties of selective laser melting AlSi10Mg alloy. Materials Science and Engineering A, 740-741**,** 148-156.

Zamani, M., Seifeddine, S., Jarfors, A. E. W., 2015. High temperature tensile deformation behavior and failure mechanisms of an Al-Si-Cu-Mg cast alloy - The microstructural scale effect. Materials and Design, 86**,** 361-370.

Zhai, Z., Pan, W., Liang, B., Liu, Y., Zhang, Y., 2022. Cracking Behavior, Microstructure and Properties of Selective Laser Melted Al-Mn-Mg-Sc-Zr Alloy. Crystals, 12.

Zhang, H., Zhu, H., Nie, X., Yin, J., Hu, Z., Zeng, X., 2017. Effect of Zirconium addition on crack, microstructure and mechanical behavior of selective laser melted Al-Cu-Mg alloy. Scripta Materialia, 134**,** 6-10.

Zhao, J., Easton, M., Qian, M., Leary, M., Brandt, M., 2018. Effect of building direction on porosity and fatigue life of selective laser melted AlSi12Mg alloy. Materials Science and Engineering: A, 729**,** 76-85.